Multi-Layer Computation of Coupled Finite Volume Solution of Depth-Averaged Flow in Steep Chute Spillways Considering Air Concentration Effects

SAEED-REZA SABBAGH-YAZDI*, HABIB REZAEI-MANIZANI **
Civil Engineering Department,
KN Toosi University of Technology,
No.1346 Valiasr Street, 19697- Tehran, IRAN
* SYazdi@kntu.ac.ir ,** Rmanizani@yahoo.com

and

NIKOS E. MASTORAKIS
Military Insitutes of University Education (ASEI)
Hellenic Naval Academy
Terma Chatzikyriakou 18539,
Piraues, GREECE mastor@wseas.org

Abstract: The results of numerical analyzing of air concentration distribution in the AVIMORE chute spillway are presented in this paper. In order to solve this phenomenon three modeling strategies are used: 1) Solving the flow parameters without considering the effects of free surface aeration and then computing air mean concentration by a separate post-processor. 2) Simultaneous solution the flow equations and computation of the air entrainment from the water free surface. 3) Adding the effects of variation in aerated water density to the numerical flow solver. Therefore, firstly, the free surface air entrainment mechanism on chute reviewed, and then, the numerical solution of shallow water equations in inclined coordinate system is described. The equations are converted to discrete form using the overlapping cell vertex and cell centre finite volume methods on a triangular unstructured mesh. The post-processor in the 1st modeling strategy uses relations for computing the inception point characteristics and air mean concentration as vertical well as distribution profiles along the chute. In the second modeling strategy the effects of free surface aeration on the bed friction coefficient reduction and depth bulking are considered at each computational step of flow solution. In the 3rd modeling strategy the effect of the water-air density variations is added to the momentum equations. The results are compared with observations on the AVIMORE chute spillway. Finally, the best experimental relations for simulating the entrainment of air into the flow on chute spillways have been chosen. In order to provide better understanding of the velocity and air concentration, the vertical distribution profiles of these parameters are plotted from the multi layer treatments of depth averaged computed results.

Key-Words: NASIR Flow Solver, Depth-Averaged Equations, Air Entrainment in Chutes

1 Introduction

Self-aeration is a phenomenon which can be observed in high velocity flows on spillways or in steep channels. The flow turns frothy and white with entrained air when aeration is initiated. Studies of self-aerated spillway flow have shown that the turbulent boundary layer, caused by the spillway surface, initiates air entrainment when it intersects the water surface at the "point of inception" (Keller et al., 1974). For some distance, the flow is developing, i.e., there is a net flux of air into the water. When the air bubbles are transported to their maximum depth in the water, the flow is considered fully aerated, but continues to entrain more air and thus is still developing. At some long distance along the spillway, uniform conditions are approached. Thereafter, there is no significant change in the hydraulic or air transport characteristics [8].

The process of self-aeration in spillways and steep chutes has historically been of interest to hydraulic engineers because of the "bulking" effect the

entrained air has on the depth of flow (Hall, 1943). The amount of "bulking" is a necessary design parameter in determining the height of spillway or chute sidewalls. Engineers have also been interested in eliminating or minimizing cavitations damage caused by high velocity flow in spillways, chutes, and channels (Falvey, 1990)[8].
The objective of this paper is modeling of the AVIMORE chute spillway. The results have been compared with data observation on the AVIMORE chute spillway. (Cain 1987)

2 Flow Regimes on Chutes

When water particles move perpendicular to the main flow direction, they must have an adequate kinetic energy to overcome the restraining surface tension to be ejected out of the flow. Volkart (1980) described the general method with droplets being projected above the water surface and than falling back, thereby entraining air bubbles into the flow. A flow is considered fully turbulent if boundary layer thickness along the chute is equal to the flow depth. In high velocity flows on spillways, the turbulent boundary layer reaches the flow surface at the "point of inception", initiating air entrainment into the flow stream. Observations have shown that there is a developing flow region after the inception point of air entrainment. For some distance in the developing region, there is a region of partially aerated flow, until the air bubbles penetrate to their maximum depth in the water and the flow becomes fully aerated. After the developing region, there is a fully developed aerated flow region where uniform conditions have been obtained[8].

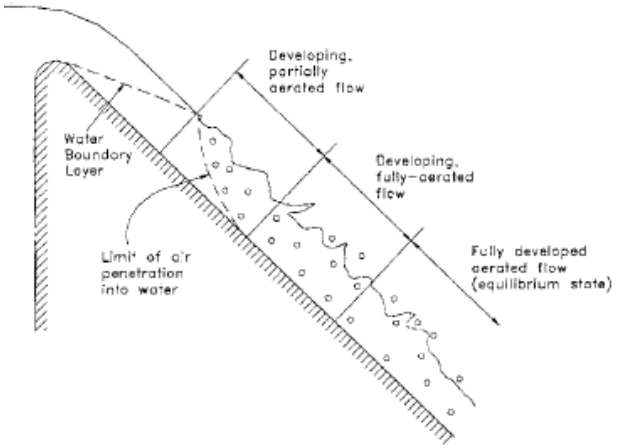

Fig.1: Region of developing flow (Keller et al., 1974).

3 Mathematical Model

3.1 Flow Equations

The water phase mathematical equations are shallow water equations modified for a coordinate system with an axis normal and two axes(x' and y) parallel to the bed surface.

$$\frac{\partial h'}{\partial t}+\frac{\partial (h'u')}{\partial x'}+\frac{\partial (h'v)}{\partial y}=0 \qquad \text{(1-a)}$$

$$\frac{\partial (h'u')}{\partial t}+\frac{\partial (u'h'u')}{\partial x'}+\frac{\partial (vh'u')}{\partial y}+\frac{\partial}{\partial x'}\left[h'\frac{gh'/\cos\alpha}{2}\right]$$
$$=gh'Sin\alpha-gh'S_{fx'} \qquad (1-b)$$

$$\frac{\partial (h'v)}{\partial t}+\frac{\partial (u'h'v)}{\partial x'}+\frac{\partial (vh'v)}{\partial y}+\frac{\partial}{\partial y}\left[h'\frac{gh'/\cos\alpha}{2}\right]$$
$$=-gh'S_{fy} \qquad (1-c)$$

In which:

$$S_{fx'}=\frac{n^2u'\sqrt{u'^2+v^2}}{h'^{4/3}}$$
$$S_{fy}=\frac{n^2v\sqrt{u'^2+v^2}}{h'^{4/3}} \qquad (2)$$

In these equations x' is the axis tangential to the chute slope and y is the same as the y axis in the global coordinate system; u' and v are the velocity components in x' and y directions, respectively; h' is the flow depth perpendicular to the chute bed surface and g is gravity acceleration; α is the chute angle; $S_{fx'}$ and S_{fy} are the bed surface friction slopes in x' and y directions, respectively and n is Manning's friction coefficient [9].
Note that the effect of density variations of water-air mixture can be considered by adding …. and …. terms to the x' and y momentum equations, respectively.

3.2 Air Concentration Relations

Wilhelm's et al. (2005) gave a relationship for defining mean air concentration [12]:

$$\overline{C}_e=\overline{C}_\infty(1-e^{-0.010X^*/Y_I}) \qquad (3)$$

Where $\overline{C}_e$ is the mean air concentration, x^* is the distance from inception point along the chute slope, Y_i is the flow depth at the point of inception, and $\overline{C}_\infty$ as follows:

$$\overline{C}_\infty=0.626(1-e^{-0.0356(\theta-10.9)})+0.23 \quad ;11\le\theta\le 75 \qquad (4)$$

Where θ is the chute angle.

Air concentration profiles *C(y)*, by Chanson (1997) expressed by[9]:

$$C = 1 - \tanh^2(K' - \frac{y'}{2D'}) \quad (5)$$

Where $; y' = \frac{Y}{Y_{90}}$

To define K' and D', the following relationships have been fit to experimental data:

$$D' = 3.5722C_e^3 - 2.3456C_e^2 + 1.15799C_e - 0.0166 \quad (6)$$

$(R^2 = 0.999)$

$$K' = 0.7766C_e^{-0.9877} \qquad (R^2 = 0.9978) \quad (7)$$

The relations used for defining the inception point distance from the crest along the chute are as follows.

Wood et al (1983) derived[2]:

$$\frac{L_{b1}}{K_s} = 13.6(Sin\alpha)^{0.0796}(F_*)^{0.713} \quad (8)$$

Where $; F_* = \frac{q_w}{\sqrt{gK_S^3 Sin\alpha}}$

Fernando et al (2002) derived

$$L_{b1} = \left(\frac{q}{0.05642k_s^{0.056}(\sin\alpha)^{0.34}}\right)^F \quad (9)$$

Where $; F = (1.46443k_s^{0.0054}(\sin\alpha)^{0.0027})^{-1}$

Where L_{b1} is the inception point distance from the crest along the chute are as follows, K_s is equivalent sand roughness, q_w is specific water discharge and α is the chute angle.

The relations used for defining the mixture flow depth at the point of inception are as follows.

Wood et al (1983) derived[2]:

$$\frac{d_{b1}}{K_S} = \frac{0.223}{(\sin\alpha)^{0.04}}(F_*)^{0.643} \quad (10)$$

Where d_{b1} is depth at the point of inception and $F_* = \frac{q_w}{\sqrt{gK_S^3 Sin\alpha}}$.

The reduction coefficient is defined by the following relation proposed by Wood et al (1991):

$$f = -2.144C^2 + 0.335C + 0.99 \quad (11)$$

4 Numerical Solution & Flow Equation

In the numerical model (1&2), the shallow water equations have been modified for a coordinate system with an axis normal and two axes(x' and y) parallel to the bed surface. The depth and velocity values are depth-averaged values computed on a triangular unstructured mesh using the finite volume method. The equations have been converted to discrete form using the overlapping cell vertex and cell centre method. The experimental relations have been added to the model to compute the inception point distance from the crest, the flow depth in this section and the depth-averaged air concentration in each joint. Then the velocity and air concentration distributions in flow depth have been obtained using experimental relations. Can write the formed vector in before stage the shallow water equations:

$$\frac{\partial Q}{\partial t} + \frac{\partial E}{\partial x} + \frac{\partial F}{\partial y} = S \quad (12)$$

4.1 Finite Volume Formulation

Application of the Green' theorem in equation (12) and the integrated equation form is:

$$\int_\Omega \left(\frac{\partial Q}{\partial t} + \frac{\partial E}{\partial x} + \frac{\partial F}{\partial y}\right) dxdy = \int_\Omega S dxdy \quad (13)$$

$$Q^{n+1} = Q^n - \frac{\Delta t}{\Omega}\sum_{k=1}^{N}\left(\overline{E}\Delta x - \overline{F}\Delta y\right)_k + S\Delta t \quad (14)$$

Where Ω is the area of the control volume , Q^{n+1} is the value of Q^n to be computed after Δt and N depend of the finite volume method(overlapping cell vertex and cell centre method).

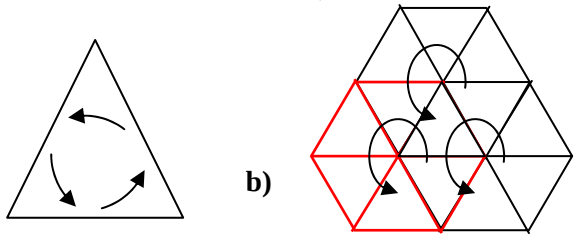

Fig.2: control volume,
a) cell centre b) overlapping cell vertex

In the cell centre method solves the governing equations for the centre of each triangular cell as a control volume. Therefore in equation (15-c) N is the number of boundary sides of the triangular cell and the flow parameters are solved at centre of the cell. Therefore, the computed parameters should be transferred to the nodal points of the cell sides.

In the cell vertex method, each control volume is formed by gathering the cells sharing a node. Therefore, N in equation (15-c) coincides with the number of triangular cells inside each control volume [9].

4.2 Boundary Conditions

Free slip impermeable condition is considered along side wall boundaries by enforcing zero normal velocity components (at nodal points of the wall edges).

The flow type in the outflow boundary is free from imposing flow parameters and upstream velocity and depth is imposed at inflow boundary. Therefore, inflow boundary conditions are imposed manually, by imposing following flow parameters:

$$u_0 = 11.07 \frac{m^2}{s} \quad , \quad h_0 = 0.2m$$

5 Three Modeling Strategies

In order to compute the average air concentration distribution using the depth average water flow parameters, three modeling strategies are used:

1) Solving the flow parameters without considering the effects of free surface aeration and then computing air concentration profiles by a separate post-processor. In this strategy the air concentration distribution is computed after completion of the numerical solution of governing equation for the water flow.

2) Simultaneous computation of the free surface aeration flow parameter (air concentration) and solving the flow equation. In this strategy the effect of aeration (i.e. reduction in global stresses and depth bulking) on flow parameters are considered at each computational step of numerical solution.

3) Adding the effects of variation in aerated water density to the numerical flow solver.

6 Simulated Results

Air concentration and velocity compared with data observation in stations 501, 503 and 505 of Aviemore spillway, with distances of 6.4, 15 and 23.6 *m* from the crest of the spillway (Fig.3).

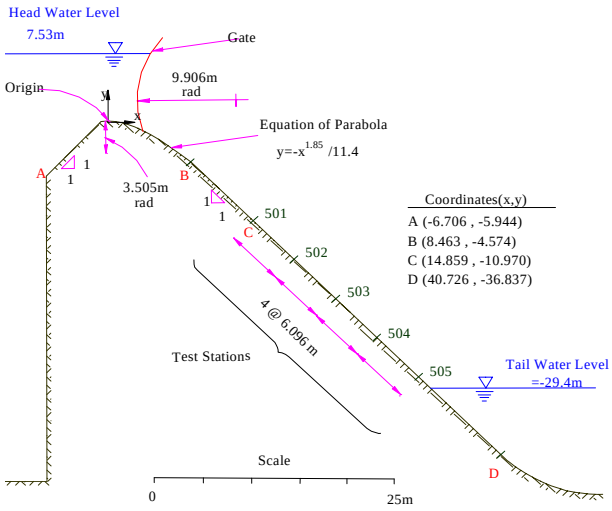

Fig.3: Aviemore spillway and measuring stations

6.1 Flow Solver Results

Figure 4 shows the triangular unstructured mesh utilized for finite volume solution of flow parameter of Aviemore spillway chute. This mesh includes 377 nodes, 642 triangular and 1018 edges.

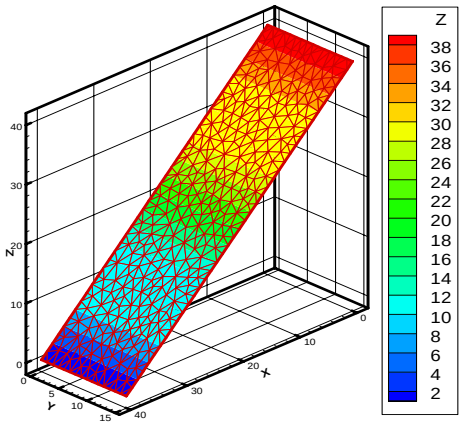

Fig.4: Mesh for Aviemore spillway chute

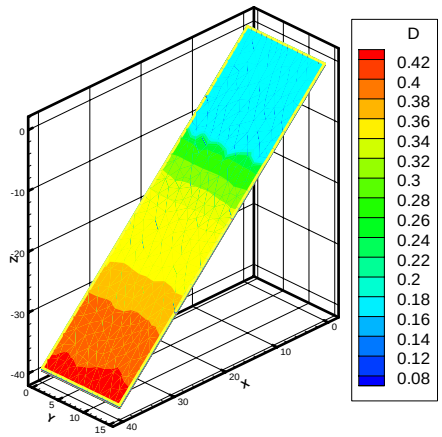

Fig.5: Depth color coded map for Aviemore spillway chute (computed by the first modeling strategy)

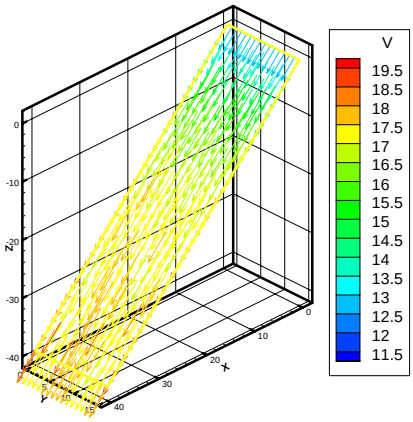

Fig.6: Velocity color coded map for Aviemore spillway chute flow (computed by the first modeling strategy)

Figures 5 and 6 show color coded maps of depth and depth averaged velocity vectors on aerated flow in the Aviemore chute spillway.

6.2 Inception Point of Aeration

The errors on the computing the location of the inception point and the flow depth in that section are tabulated in the following tables.

Table 1: Errors on computed inception point distance from the starting point of super critical flow (1st modeling strategy)

Finite Volume Method	Fernando et al (2002)		Wood et al (1983)	
	Value (m)	Errors	Value (m)	Errors
Overlapping Cell Vertex	11.77	15.96%	8.26	41%
Cell Centre	12.67	9.5%	8.71	37.8%

Table 2: Errors of computed depth at inception point (1st modeling strategy)

Finite Volume Method	Bauer (1954)		Wood et al (1983)	
	Value (m)	Errors	Value (m)	Errors
Overlapping Cell Vertex	0.122	19.74%	0.157	3.29%
Cell Centre	0.135	11.18%	0.166	9.21%

Table 3: Errors on computed inception point distance from the starting point of super critical flow (2nd modeling strategy)

Finite Volume Method	Fernando et al (2002)		Wood et al (1983)	
	Value (m)	Errors	Value (m)	Errors
Overlapping Cell Vertex	14.85	6.07%	11.41	18.50%
Cell Centre	14.78	5.57%	11.37	18.79%

Table 4: Errors of computed depth at inception point (2nd modeling strategy)

Finite Volume Method	Bauer (1954)		Wood et al (1983)	
	Value (m)	Errors	Value (m)	Errors
Overlapping Cell Vertex	0.125	17.76%	0.134	11.84%
Cell Centre	0.136	10.53%	0.142	6.58%

Table 5: Errors on computed inception point distance from the starting point of super critical flow (3rd modeling strategy)

Finite Volume Method	Fernando et al (2002)		Wood et al (1983)	
	Value (m)	Errors	Value (m)	Errors
Overlapping Cell Vertex	14.85	6.07%	11.40	18.57%
Cell Centre	14.78	5.57%	11.37	18.79%

Table 6: Errors of computed depth at inception point (3rd modeling strategy)

Finite Volume Method	Bauer (1954)		Wood et al (1983)	
	Value (m)	Errors	Value (m)	Errors
Overlapping Cell Vertex	0.125	17.76%	0.134	11.84%
Cell Centre	0.132	13.16%	0.142	6.58%

By comparison between the mean air concentration computed by three modeling strategies, it can be concluded that the best relation for inception point distance and depth are those proposed by Fernando's and Wood's, respectively.

6.3 Mean Air Concentration

Figure 7 shows the field measurement of the air concentration profile in flow depth in station 503 [4]. The mean air concentration is computed by integrating on the air concentration profile at that station.

$$c_{mean} = \frac{1}{h}\int_0^h cdh$$

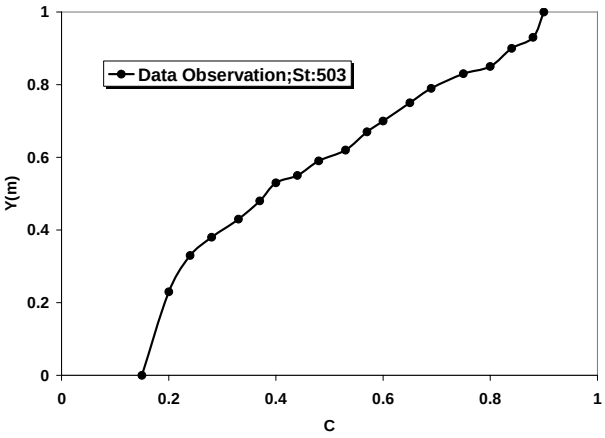

Fig.7 Air concentration - flow depth in station 503 [5]

Table7: Errors on computed mean air concentration (for three modeling strategies)

Finite Volume Method	Overlap cell vertex		Cell centre	
	Value	Errors	Value	Errors
1st modeling strategy	0.46%	3.03%	0.45%	0.92%
2nd modeling strategy	0.454%	1.91%	0.445%	0.25%
3rd modeling strategy	0.454%	1.91%	0.445%	0.25%

6.4 Mean Aerated Flow Velocity

Figure 8 shows the field measurement of the velocity profile in flow depth in station 503 [4]. Here the mean velocity is computed by integrating on the velocity profile at that station.

$$V_{mean} = \frac{1}{h}\int_0^h vdh$$

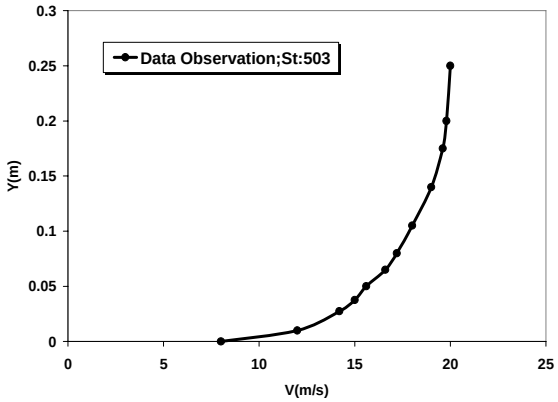

Fig. 8 Velocity - flow depth in station 503 [5]

Table8: Errors on computed average velocities (for three modeling strategies)

Finite Volume Method	Overlap cell vertex		Cell centre	
	Value (m/s)	Errors	Value	Errors
1st modeling strategy	14.41	18.35%	16.90	4.22%
2nd modeling strategy	17.00	3.65%	17.79	0.8%
3rd modeling strategy	17.01	3.61%	17.8	0.86%

Comparison of the velocity values computed by 2nd and 3rd strategies shows that consideration of the water-air density variations in the momentum equations produces negligible differences in computed average velocities.

Since the cell center finite volume method produces better results than the cell vertex finite volume method, cell centre scheme will be used for the rest of the work of this paper.

6.5 Air Concentration Profiles Computation

To choose the best relation for defining mean air concentration in three modeling strategies the program has been run for the case of using Fernando's relation for distance inception point and Wood's relation for depth inception point. Here, the program is run for the case of using Fernando's relation for inception point location, Wood's relation for flow depth at the point of inception, and Wilhelm's relation for mean air concentration.

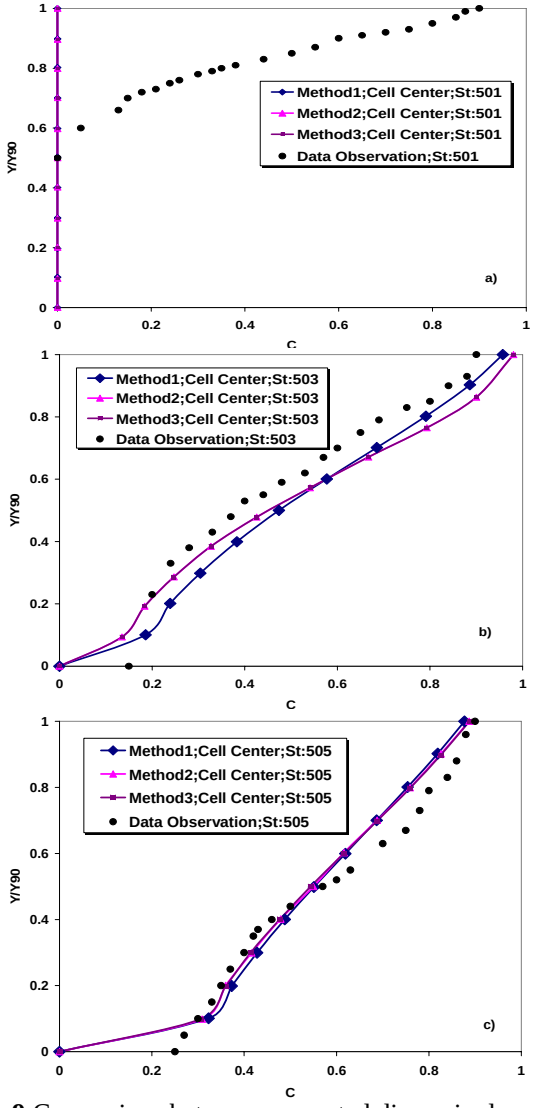

Fig.9 Comparison between computed dimensionless air concentration (using cell center scheme) and data observation as function of dimensionless flow depth (a: St=501, b: St=503, c: St=505)

6.6 Velocity Profiles Computation

The relation used for defining velocity profiles in flow depth, as follows:

$$V_{mean} = \frac{V_I}{Y_I^{n+1/n}} \int_0^{Y_{max}} Y^{1/n} dy \quad ; \quad n = 6$$

Where y_{90} is the characteristic mixture depth with local air concentration of C=0.90 and u_{90} is the mixture surface velocity.

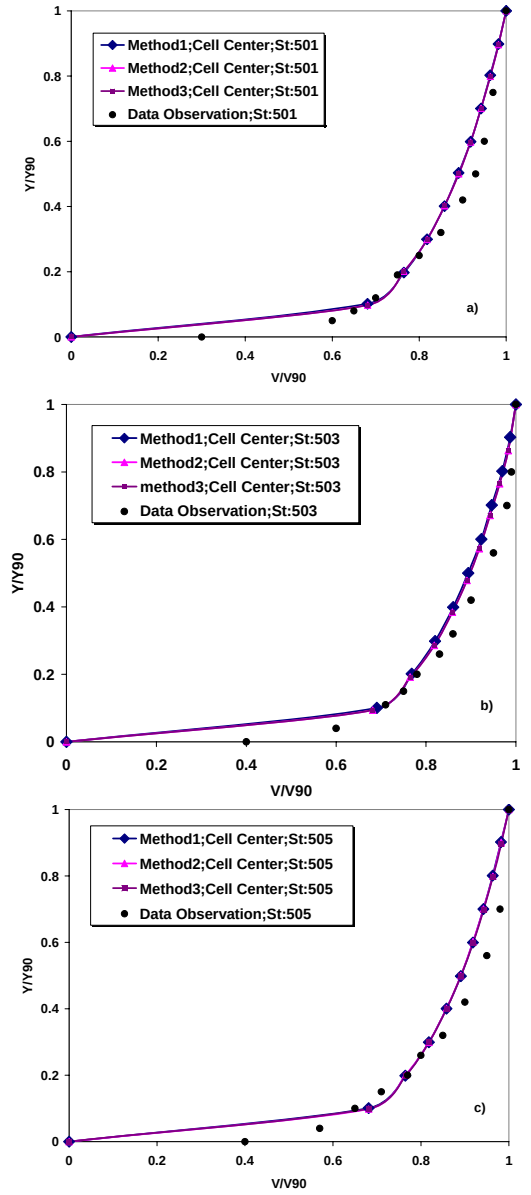

Fig.10 Comparison between computed dimensionless velocity (using cell center scheme) and data observation as function of dimensionless flow depth (a: St=501, b: St=503, c: St=505)

7. Conclusion

The numerical solution of flow on steep chute spillway has been carried out using shallow water equations modified in inclined coordinate system. Experimental relations have been used for computing distribution of mean air concentration using the results of the numerical flow solver. The numerical solution of the flow equations were performed using two finite volume methods in which the control volume (CV) were chosen as a triangular cell (cell centre CV) and summation of triangles meeting at each computational node (cell vertex CV).

Computation of mean air concentration in the AVIMORE chute spillway are performed using three modeling methods 1) Solving the flow parameters without considering the effects aeration from the water surface and then computing mean air concentration by a separate post-processor. 2) Simultaneous computing the free surface aeration and solving the flow equations at each computational step (by considering reduction in global stresses and flow depth bulking) and 3) Considering the effects of density variation in numerical solution of aerated flow.

The comparison of the results of two modeling strategies with the field measurements ends up with following conclusions:

- Relation 9 for defining inception point location (proposed by Fernando 2002) matches nicely with the utilized flow solver.
- Relation 10 for defining flow depth at the inception point (proposed by Wood 1983) produces good results in conjunction with the utilized flow solver
- Simultaneous computing the mean air concentration and solving the flow equations at each computational step results in more accurate computation of average velocity.
- Using cell centre finite volumes for the solution of the flow equations provides acceptable results for average velocity (by considering air concentration effects).
- Solving depth average flow equations (even with simple turbulent models like zero equation model) can produce realistic results when the effects air concentration on global stresses reduction and flow depth bulking are considered.
- Comparison of the computed velocities shows that the effect of water-air density variations on formation of computed flow parameters is negligible.

References:

[1] Bauer WJ (1954) Turbulent Boundary Layer on Steep Slopes. Transaction,ASCE,Vol.119, No.2719: 1212-1242

[2] Cain P & Wood IR.(1983) Measurements of Self- Aerated Flow on Spillways. J. of Hyd. Div., 107, HY11: 1425-1444

[3] Chanson H (1988) Study of Air Entrainment and Aeration Devices on Spillway Model. A Thesis Submitted in Partial Fulfillment of the Requirements for the Degree at the University of Canterbury, New Zealand

[4] Chanson H (1995) Air Concentration Distribution in Self-Aerated Flow - Discussion. Journal of Hydraulic Engineering. Res., IAHR, Vol. 33, No. 4 : 586-588 (ISSN 0022-1686).

[5] Chanson H (1994) Air-Water Interface Area in Self-Aerated Flow. Water Res., IAWPRC, Vol. 28, No. 4: 923-929 (ISSN 0043-1354).

[6] Chanson H (1993) Self-Aerated Flows on Chutes and Spillways. Journal of Hydraulic Engineering, ASCE, Vol. 119, No. 2, pp. 220-243. Discussion: Vol. 120, No. 6: 778-782 (ISSN 0733-9429).

[7] Chanson H (1992) Uniform Aerated Chute Flow - Discussion. Journal of Hydraulic Engineering, ASCE, Vol. 118, No. 6: 944-945 (ISSN 0733-9429).

[8] Kramer K(2004) Development of Aerated Chute Flow. Doctoral Thesis ETH No. 15428; Dipl.-Ing. Technical University of Darmstadt (TUD).

[9] Sabbagh-Yazdi SR , Mastorakis EN & Zounemat-Kermani M (2007) Velocity Profile over Spillway by Finite Volume Solution of Slopping Depth Averaged Flow. 2nd IASME/WSEAS International Conference on Continuum Mechanics, Protozoa (Porto rose), Slovenia, May 15-17

[10] Sabbagh-Yazdi SR & SaeediFar B (2007) Analyses of Two-Dimensional Turbulence Flow in Channel With Sudden Explanation by Using Cell Centre Finite Volume Method 32nd Congress of IAHR , The International Association of Hydraulic Engineering, Venice, Italy

[11] Sabbagh-Yazdi, SR (2006) Spillway Flow Modeling by Finite Volume Solution of Slopping Depth Averaged Equations on Triangular Mesh; Application to KAROUN-4. 10th WSEAS International Conference on Applied Mathematics, Dallas (Texas), USA

[12] Sabbagh-Yazdi SR, Zounemat-Kermani M and Mastorakis NE (2007) Velocity Profile over Spillway by Finite Volume Solution of Sloping Depth Averaged Flow. WSEAS Journal of Applied and Theoretical Mechanics, Issue 3, Vol.2,85-94

[13] Wilhelm S (2005) Bubbles and Waves Description of Self-Aerated Spillway Flow. Journal of Hydraulic Research Vol. 43, No. 5: 522-531